Although the coarseness of the grid used in this example precludes quantitative comparisons, the qualitative features of these results are in agreement with those obtained experimentally and theoretically using an approximate continuum solution for similar torsion problems.[3]

The purpose of this Note is solely to demonstrate a stable algorithm for finite element analysis of partly wrinkled membranes. Questions concerning accuracy and rate of convergence in realistic technological applications are currently under investigation and will be addressed in future publications.

Acknowledgment

Funding for this research was provided by the Jet Propulsion Laboratory, California Institute of Technology, under Contract 955873.

References

[1] Stein, M. and Hedgepeth, J.M., "Analysis of Partly Wrinkled Membranes," NASA TN D-813, July 1961.

[2] Mikulas, M.M. Jr., "Behavior of Doubly Curved Partly Wrinkled Membrane Structures Formed from an Initially Flat Membrane," Ph.D. Thesis, Virginia Polytechnic Institute, Blacksburg, Va., June 1970.

[3] Mikulas, M.M. Jr., "Behavior of a Flat Stretched Membrane Wrinkled by the Rotation of an Attached Hub," NASA TN D-2456, Sept. 1964.

[4] Zienkiewicz, O.C., *The Finite Element Method*, 3rd ed., McGraw-Hill, London, 1977, pp. 93-118.

AIAA 82-4294

Load-Frequency Relations for a Clamped Shallow Circular Arch

Eric R. Johnson*

Virginia Polytechnic Institute and State University, Blacksburg, Virginia

Introduction

THE subject of this Note is the infinitesimal free vibration of a shallow circular arch about a nonlinear, prebuckled, static equilibrium configuration. The arch is elastic, its ends are clamped a fixed distance apart, and its motion is assumed to occur in its plane of curvature. It is subjected to a spatially uniform static load which can cause snap through to an inverted configuration. On a load-deflection equilibrium path, snap-through instability occurs either at a limit point (relative maximum load) or at a bifurcation point (intersection of equilibrium paths).

The results are presented as characteristic curves that are plots of the static load magnitude vs the square of the frequencies. The curve corresponding to the lowest frequency is called the fundamental characteristic curve. This curve intersects the frequency (squared) axis at the fundamental natural frequency, and intersects the load axis (zero frequency) at the snap-through load. For the arch problem considered here, the fundamental characteristic curve is concave toward the origin. This property is useful in estimating the fundamental natural frequencies, and in approximating the snap-through load experimentally but nondestructively. If the snap-through load and the fundamental natural frequency at zero load are known, then a straight line connecting these points in the characteristic plane provides a lower bound to the fundamental natural frequencies at intermediate load levels. If the fundamental natural frequencies are determined experimentally at two static load magnitudes, these results may be used to construct a straight line extrapolation to the load axis (zero frequency). This load is an upper bound to the snap-through load.

This Note is a summary of a report by the author and R. H. Plaut,[1] and is a supplement to Ref. 2 on the load-frequency relations for three shallow elastic structures, one of which is a pinned-end circular arch subject to a uniform load. Many authors have considered the free vibrations of columns, plates, and shells (see the bibliographies in Refs. 3 and 4). Fewer papers exist for shallow elastic structures.

Received Nov. 23, 1981; revision received March 25, 1982.

*Assistant Professor, Aerospace and Ocean Engineering. Member AIAA.

Analysis

The shallow arch shown in Fig. 1 is homogeneous and has a uniform cross section. The unloaded configuration (dashed-dotted line) is denoted $Y_0(X)$, the equilibrium configuration under the distributed load $Q(X)$ is $Y_s(X)$, and the configuration at time T is $Y(X,T)$. Also, μ denotes the mass per unit length, E Young's modulus, I the moment of inertia of the cross section, and A the cross-sectional area.

Define the nondimensional quantities

$$x=\frac{X}{L},\quad y=\frac{Y}{2}\sqrt{\frac{A}{I}},\quad y_0=\frac{Y_0}{2}\sqrt{\frac{A}{I}},\quad y_s=\frac{Y_s}{2}\sqrt{\frac{A}{I}}$$

$$t=\pi^2 T\sqrt{\frac{EI}{\mu L^4}},\quad q=\frac{QL^4}{2\pi^4 EI}\sqrt{\frac{A}{I}} \tag{1}$$

Let dots and primes denote partial differentiation with respect to t and x, respectively. The equation of motion is

$$\pi^4\ddot{y}+y''''-y_0''''+2y''\int_0^1[(y_0')^2-(y')^2]\mathrm{d}x=-\pi^4 q \tag{2}$$

in which axial and rotatory inertia terms are neglected. Setting the time derivative term (lateral inertia) to zero in Eq. (2) reduces it to the static equilibrium equation derived in Ref. 5. The nonlinear term in Eq. (2) represents the geometric coupling between bending and axial thrust due to large deflections. In this term the definite integral is proportional to the axial thrust, which is spatially uniform since the curvature is small. The boundary conditions are

$$y=0,\quad y'=y_0' \text{ at } x=0,\ 1, \text{ and } t>0 \tag{3}$$

The equilibrium configuration satisfies the equation

$$y_s''''-y_0''''+\gamma^2 y_s''=-\pi^4 q \tag{4}$$

where the induced thrust is

$$\gamma^2=2\int_0^1[(y_0')^2-(y_s')^2]\mathrm{d}x \tag{5}$$

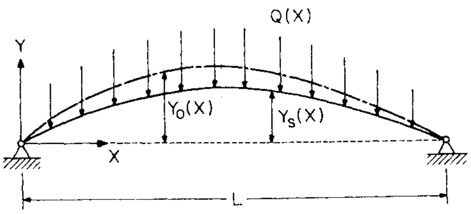

Fig. 1 Shallow arch.

Let $w(x,t)$ denote the motion about $y_s(x)$, i.e., $w(x,t) = y(x,t) - y_s(x)$. Subtracting Eq. (4) from Eq. (2) yields the equation of motion for w. If this equation is linearized and vibrations of the form $w(x,t) = z(x)\exp(i\omega t)$ are considered, one obtains

$$z'''' + \gamma^2 z'' - \pi^4 \omega^2 z = 4y_s'' \int_0^1 z' y_s' \mathrm{d}x \tag{6}$$

The boundary conditions on the vibration modes are $z = z' = 0$ at $x = 0$ and $x = 1$.

Consider:

$$y_0(x) = 4cx(1-x), \quad q(x) = q_0, \quad c > 0, \quad q_0 > 0 \tag{7}$$

which represents a circular initial shape for a shallow arch with a nondimensional height c at midspan, subject to a uniformly distributed load. The symmetric solution of Eq. (4) subject to boundary conditions, Eq. (3), is

$$y_s(x) = 4c(\alpha - 1)\{\cot(\gamma/2)[1 - \cos\gamma x] - \sin\gamma x\}/\gamma \tag{8}$$

if $\gamma \neq 0$ or $\gamma \neq 2n\pi$, $n = 1, 2, \ldots$, and where

$$\alpha = \pi^4 q_0 / (8c\gamma^2) \tag{9}$$

(Solutions for $\gamma = 0$ or $\gamma = 2n\pi$ are in Ref. 1.) Substituting Eqs. (7) and (8) in Eq. (5) requires α to be a root of

$$A\alpha^2 + B\alpha + C - \gamma^2/(32c^2) = 0 \tag{10}$$

where

$$A = -5/6 + 8/\gamma^2 - 3\cot(\gamma/2)/\gamma - \cot^2(\gamma/2)/2$$

$$B = 1 - 8/\gamma^2 + 2\cot(\gamma/2)/\gamma + \cot^2(\gamma/2)$$

$$C = -1/6 + \cot(\gamma/2) - \cot^2(\gamma/2)/2 \tag{11}$$

If c is sufficiently large, there are also asymmetric solutions to Eqs. (3-5) which bifurcate from the symmetric solution Eq. (8) on the load-deflection path.

For free vibrations about the static equilibrium configuration Eq. (8), Eq. (6) is solved to determine the mode shapes and frequencies. The solutions separate into inextensible (antisymmetric) modes and extensible (symmetric) modes depending on whether the right-hand side of Eq. (6) vanishes or not. The integral factor on the right-hand side of Eq. (6) is proportional to the amount of additional extension or contraction of the centerline during vibration. The inextensible modes are

$$z_n(x) = A_n\{\sin[r_{2n}(2x-1)] - G_n \sinh[r_{1n}(2x-1)]\} \qquad n = 2, 4, \ldots \tag{12}$$

where

$$r_{1n}^2 = [-\gamma^2 + (\gamma^2 + 4\pi^4\omega_n^2)^{1/2}]/8$$

$$r_{2n}^2 = [\gamma^2 + (\gamma^2 + 4\pi^4\omega_n^2)^{1/2}]/8$$

$$G_n = r_{2n}\cos r_{2n} / (r_{1n}\cosh r_{1n}) \tag{13}$$

The associated frequencies are the roots of

$$r_{2n}\cos r_{2n}\tanh r_{1n} - r_{1n}\sin r_{2n} = 0 \tag{14}$$

The extensible modes are

$$z_n(x) = A_n\{\cos[r_{2n}(2x-1)] - E_n\cosh[r_{1n}(2x-1)] - F_n y_s''(x)/(8c)\} \qquad n = 1, 3, \ldots \tag{15}$$

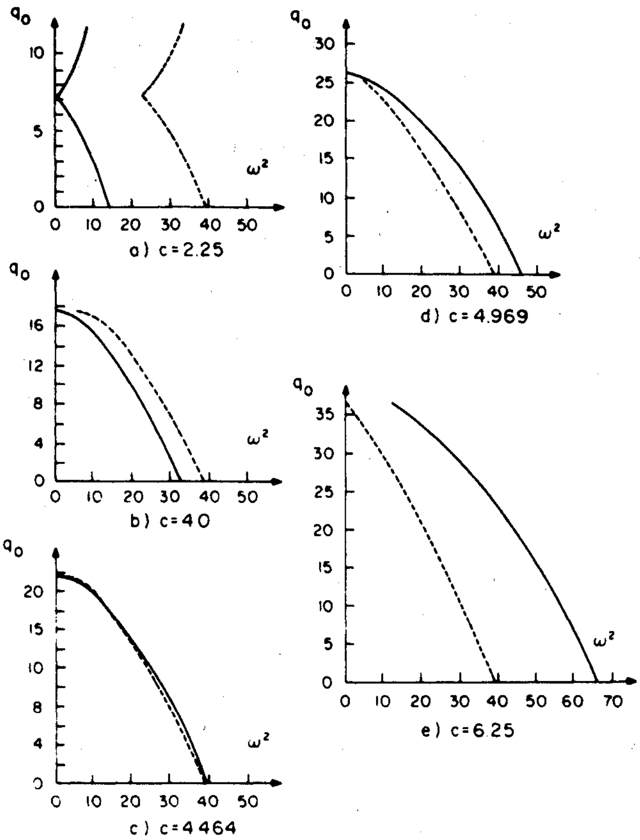

Fig. 2 Characteristic curves for increasing values of the dimensionless midspan height.

where coefficients E_n and F_n are given in Ref. 1. The frequencies of the extensible modes are the roots of

$$(C_{1n} + C_{3n}\tanh r_{1n})\cos r_{2n} + (C_{2n} + C_{4n}\tanh r_{1n})\sin r_{2n} = 0 \tag{16}$$

Coefficients C_{1n}, C_{2n}, C_{3n}, and C_{4n} are given in Ref. 1. The static equilibrium configuration influences the mode shapes, Eqs. (12) and (15); however, their shapes do not vary significantly with the load.

Numerical Results and Discussion

Characteristic curves for ω_1^2 (solid lines) and ω_2^2 (dashed lines) are presented in Figs. 2a-e for different values of the arch rise parameter c. If $0 < c < (\pi/2)^2$, the load-deflection path is monotonic and no instability occurs, so the frequencies remain positive as in Fig. 2a. If $(\pi/2)^2 < c < 4.969$, the arch becomes unstable at a limit point. At the limit point load, ω_1 becomes zero and the characteristic curves have zero slope as in Figs. 2b and 2c. If $c = 4.969$, bifurcation occurs at the limit point and the first two frequencies vanish simultaneously (Fig. 2d). If $c > 4.969$, bifurcation instability occurs before the equilibrium path reaches the limit point and ω_2 is zero at the critical load (Fig. 2e).

In the range $4.464 < c < 4.969$, the first two characteristic curves intersect between $q_0 = 0$ and the critical load (limit point). The smaller value of c corresponds to the coincidence of ω_1 and ω_2 at $q_0 = 0$. The fundamental characteristic curve consists of ω_2^2 to the intersection point and then ω_1^2 to the critical load (Fig. 2c), and the mode switches from an antisymmetric shape to a symmetric shape. It is noted[2] that for pinned-end conditions and $2.296 < c < 2.690$, the fundamental curve consists of ω_1^2 from $q_0 = 0$ to the intersection point and ω_2^2 to the critical load (bifurcation point), and the mode shape changes from symmetric to antisymmetric. Hence, assuming the first two characteristic curves intersect between $q_0 = 0$ and the critical load, the order in which they comprise the fundamental curve as the load increases is reversed if the end conditions change from clamped to pinned.

Acknowledgment

Mr. David A. Tice performed some of the calculations.

References

[1] Johnson, E. R. and Plaut, R. H., "Load-Frequency Relationships for Shallow Elastic Arches," Virginia Polytechnic Institute and State University, Blacksburg, Va., Rept. VPI-E-80-4, Feb. 1980.

[2] Johnson, E. R., Plaut, R. H., and Deel, C. C. II, "Load-Frequency Relationships for Shallow Elastic Structures," *Recent Advances in Structural Dynamics, an International Conference*, edited by M. Petyt, University of Southampton, England, July 1980, pp. 611-620.

[3] Plaut, R. H., "Vibration Frequencies of an Arch Model Under Various Loading Conditions," Virginia Polytechnic Institute and State University, Blacksburg, Va., Rept. VPI-E-79-19, May 1979.

[4] Baruch, M., "Integral Equations for Nondestructive Determination of Buckling Loads for Elastic Plates and Bars," *Israel Journal of Technology*, Vol. 11, March 1973, pp. 1-8.

[5] Fung, Y. C. and Kaplan, A., "Buckling of Low Arches or Curved Beams," U.S. National Advisory Committee for Aeronautics, TN 2840, 1952, p. 7.

AIAA 82-4295

Second-Order Sensitivity Derivatives in Structural Analysis

Raphael T. Haftka*

Virginia Polytechnic Institute and State University, Blacksburg, Virginia

THE interest in calculating sensitivity derivatives of constraints on structural behavior is evidenced by a number of recent publications (e.g., Refs. 1-5). Most papers are concerned with calculation of first derivatives of constraints. However, a recent Note by Haug presents expressions for the calculation of second derivatives of static constraint functions. Haug's method resulted in an order-of-magnitude saving over standard methods for calculating such derivatives. The purpose of the present Note is to present a similar but simplified procedure that results in reducing the computational cost by an additional factor of two. The results are presented in a notation that is different from that of Ref. 1, but is more common in other work on structural analysis and synthesis.

The structure is assumed to be discretized by a finite element model and governed by the equation of equilibrium

$$KU = F \tag{1}$$

where K is the stiffness matrix, U is the displacement vector, and F is a load vector. The structure and therefore the displacement may be controlled by design variables. We assume that there are n design variables, but for simplicity we obtain expressions for derivatives with respect to two of these variables, x and y. A constraint on the structural response may be written as

$$g(x,y,U) \geq 0 \tag{2}$$

We are concerned with methods for computing the second derivatives of g with respect to design variables. We start by considering the first derivatives. Differentiating Eq. (2) with respect to x, we obtain

$$\frac{dg}{dx} = \frac{\partial g}{\partial x} + Z^T \frac{dU}{dx} \tag{3}$$

where the vector Z has the components $Z_i = \partial g / \partial U_i$. Differentiating Eq. (1) we obtain

$$K\frac{dU}{dx} = \frac{dF}{dx} - \frac{dK}{dx} U \tag{4}$$

It is possible to solve for dU/dx from Eq. (4) and substitute into Eq. (3), which can be written symbolically as

$$\frac{dg}{dx} = \frac{\partial g}{\partial x} + Z^T K^{-1} \left[\frac{dF}{dx} - \frac{dK}{dx} U \right] \tag{5}$$

However, when there are many design variables it may be more advantageous to define an adjoint variable Λ as the solution of

$$K\Lambda = Z \tag{6}$$

so that

$$\frac{dg}{dx} = \frac{\partial g}{\partial x} + \Lambda^T \left[\frac{dF}{dx} - \frac{dK}{dx} U \right] \tag{7}$$

where use has been made of the symmetry of the matrix K. This alternative approach is often called the "dummy load approach," with Z being the dummy load. It requires the solution of a system of equations, Eq. (6), once for each constraint function, whereas the system of Eq. (4) has to be solved once for each design variable. The dummy load approach thus has the advantage when there are more design variables than behavior constraints.

To calculate second derivatives we can differentiate Eq. (3) with respect to another design variable, y:

$$\frac{d^2 g}{dx dy} = \frac{\partial^2 g}{\partial x \partial y} + \left(\frac{\partial Z}{\partial x} \right)^T \frac{dU}{dy} + \left(\frac{dU}{dy} \right)^T R \frac{dU}{dx} + \left(\frac{\partial Z}{\partial y} \right)^T \frac{dU}{dx} + Z^T \frac{d^2 U}{dx dy} \tag{8}$$

where the term R_{ij} in the matrix R is $\partial^2 g / \partial U_i \partial U_j$. To obtain $d^2 U / dx dy$ for Eq. (8), we have to differentiate Eq. (4) with respect to y,

$$K\frac{d^2 U}{dx dy} = \frac{d^2 F}{dx dy} - \frac{d^2 K}{dx dy} U - \frac{dK}{dx}\frac{dU}{dy} - \frac{dK}{dy}\frac{dU}{dx} \tag{9}$$

Thus, each second derivative of the constraint requires solution of a system of equations, Eq. (9). When we have n design variables, we need to solve Eq. (9) $n(n+1)/2$ times and Eq. (4) n times to get all the second derivatives of g. Haug suggested a more economical approach requiring two additional adjoint vectors. For n design variables, there would be need for only $2n$ adjoint vectors and $2n$ solutions of systems of equations instead of $n + n(n+1)/2$. It is, however, possible to do much better. Substituting for $d^2 U / dx dy$ from

Received Feb. 26, 1982.

*Professor, Department of Aerospace and Ocean Engineering. Member AIAA.